

図3-2 ファージディスプレイ法によるペプチドアプタマー獲得法

① ペプチドライブラリー (PL) をコードするDNAを挿入したファージミドベクターを構築する。② *E. coli* へファージミドベクターを導入すると共にヘルパーファージを感染させる。③ g3p (gene 3 protein) にペプチドアプタマー候補を提示させたファージを出芽させる。④ 固定化した標的タンパク質 (TP) に対してペプチド提示ファージをパニングする。⑤ 標的タンパク質とペプチドアプタマーの特異的結合活性を指標にしてファージを選択・溶出する。⑥ 回収したファージは *E. coli* に再感染・増幅させる。そして、上記の③～⑥のサイクルを繰り返す、目的のペプチドアプタマーを濃縮・獲得する。

ドをコードする mRNA の 3' 末端にピューロマイシンリンカーを連結する特別な操作を必要とする。これにより、ペプチド翻訳が終了すると同時に、リボソームの P サイトにあるペプチド鎖とピューロマイシンが反応する。その結果、ペプチドと mRNA が共有結合で連結した安定な対応付け分子が形成される。また、両手法とも、対応付け分子を構築する操作以外は、すでに確立した核酸アプタマー選択法の技術をそのまま適用できることも大きな利点となっている。

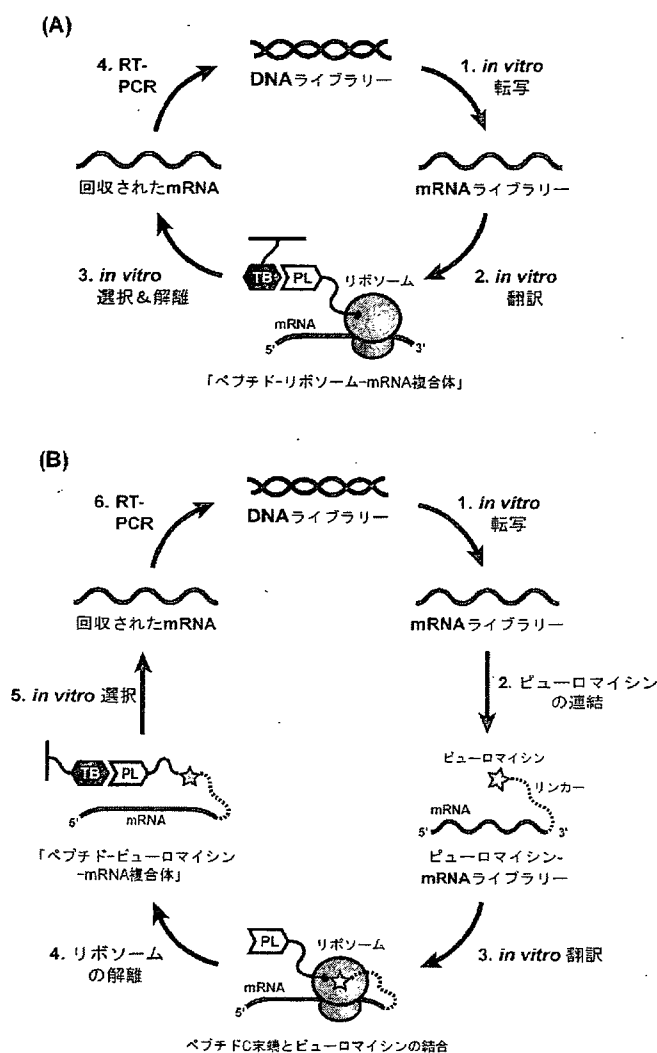


図4 新しいペプチドアプタマー獲得法

(A)リボソームディスプレイ法, (B)mRNAディスプレイ (*in vitro virus*) 法

TB: Target Biomolecule (例. タンパク質/酵素/生理活性低分子), PL: Peptide Library

## 4 アプタマーの機能化

### 4.1 安定性の向上

オリゴ核酸を医薬品として用いる際、その生体内安定性が低いことが問題点となる。通常、RNAやDNAの血中での半減期は、およそ数秒から数分である。それゆえ、核酸アプタマーの生体内安定性を高めるため、非天然核酸の導入が試みられている。これまでにも、多様な核酸誘導体が数多く開発されている(図5)。現在、非天然核酸をアプタマーに組み込む方法は主に2つある。一つは、すでに結合活性のある天然核酸アプタマーの一部を非天然核酸に置換する方法(ポスト修飾法)である。Schmidらは、抗tenasin-Cアプタマーの核酸配列の一部を、LNA

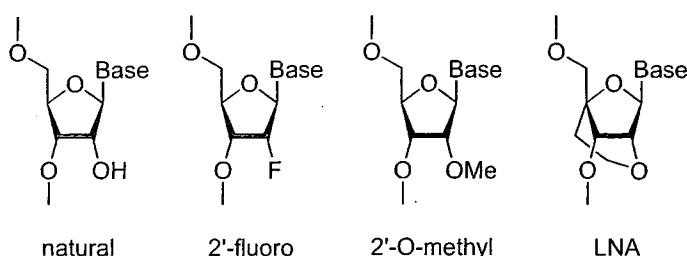


図5 核酸アプタマーへ導入された非天然核酸の例

(Locked Nucleic Acid) で置換することにより、その熱的安定性と酵素分解耐性の向上に成功した<sup>37)</sup>。

もう一つは、非天然核酸アナログをポリメラーゼの基質として、SELEX法の過程に組み込む方法である。例えば、アプタマー医薬品であるMacugen (抗VEGFアプタマー)の開発過程では、2'-位フッ素化ピリミジンアナログ及び天然プリンを用いたSELEX法が行われ、第一世代のアプタマーを獲得している。そして、ポスト修飾法により、2'位メトキシヌクレオチドを導入することで、高い生体内安定性をもつアプタマーを完成させた<sup>5)</sup>。また、松田らは、4'位硫黄化ピリミジンアナログを用いて、抗トロンビンアプタマーの創製を報告している<sup>38)</sup>。

現在、ポリメラーゼを用いて非天然核酸アナログを導入する場合、必ず起こりえる問題として、オリゴ核酸鎖への導入効率が低いことが挙げられる。そこでEllingtonらは、2'位メトキシヌクレオチドアナログを基質として効率よく鎖伸長できる変異型T7RNAポリメラーゼを開発した<sup>39)</sup>。一方、Keefeらは、変異型T7RNAポリメラーゼを用いて、すべて2'位メトキシヌクレオチドアナログ骨格からなるアプタマーをSELEX法により創出した<sup>40)</sup>。このアプタマーは、VEGFを標的としており、2'位メトキシヌクレオチドの高い生体内安定性から、Macugenに勝る有望なアプタマー医薬品となり得る。近い将来、様々な非天然核酸を含むオリゴ核酸を導入したアプタマー創製法が確立すれば、これまでに創造し得なかった新たなアプタマー医薬の誕生が期待できる。

#### 4.2 デリバリ-機能付与

一般的にウイルスが細胞に感染するとき、10から20個のアミノ酸から構成される特徴的なペプチド機能を利用することが知られている。例えば、HIV-1 (Human immunodeficiency virus type -1) のTAT<sup>41)</sup>やHSV (Herpes-simplex-virus) のVP-22<sup>42)</sup>のタンパク質配列中には、カチオン性アミノ酸 (アルギニン・リジン) に富んだペプチド配列 (PTD : Protein Transduction Domain) が存在し、哺乳類細胞の細胞膜に対して特異的に結合するだけでなく、細胞内へ能動的に侵入する機能を発現する。つまり、これらのペプチドは、ウイルスが利用する天然型の機能

性ペプチドアプタマーといえる。このPTDの細胞透過性と核移行性は、目的の組織・臓器に薬物としての低分子化合物・核酸を送達するドラッグデリバリーシステムのキャリアーとして極めて魅力的な性質であり、近年、数多くの大学・研究機関・企業が早期実用化を目指して研究に取り組んでいる<sup>43,44)</sup>。それゆえ、薬物送達のキャリアーとしてのペプチドアプタマーの開発・改良<sup>45)</sup>も、ペプチドを利用した新たな医療を開拓する重要な研究として位置づけられる。

### 4.3 機能の複合化

オリゴ核酸の特徴である配列特異性とアプタマーとしての機能を巧みに利用した新しい試みもある。それは、核酸アプタマーに対するアンチセンス核酸を用いて活性を制御するという方法である<sup>46)</sup>。例えば、トロンビンに対するアプタマーの抗血液凝固作用が強すぎる場合、生体において有害となる。このとき、アプタマーに対するアンチセンス核酸を投与すれば、アプタマーとアンチセンス核酸は二本鎖を形成し、トロンビンへの結合は阻害される。この結果、アプタマーの作用は緩和される。このように、解毒 (antidote) 機能を付与・制御する分子レベルの設計戦略は、核酸配列を有するアプタマーであるからこそ可能であったといえる。

## 5 おわりに

現在の抗体医薬は、疾病原因分子に対して特異的に作用する優れた分子標的薬として確固たる地位を築きつつある。しかし、ある頻度で治療効果の低い患者が存在することを始め、中和抗体による影響、製造に関する特許権の錯綜、高額な生産コスト等、解決すべき問題点も多く残している。一方、アプタマー医薬は、細胞内外のいずれの標的分子に対しても作用するマルチ医薬として開発することが可能であり、上記の抗体医薬に関わる諸問題を解決・補完するものとして活躍できるであろう。それゆえ、アプタマーの新規開発を支える進化分子工学的手法の更なる改善、オリゴ核酸やペプチドの生体内動態・薬効・安全性を評価するシステムの確立により、将来のアプタマー医薬によるテイラーメイド医療の実現を大いに期待したい。

## 文 献

- 1) C. Tuerk *et al.*, *Science*, **249**, 505 (1990)
- 2) AD. Ellington *et al.*, *Nature*, **346**, 818 (1990)

- 3) S. Miyakawa *et al.*, [Aptamer therapeutics], 蛋白質核酸酵素, **51**, 2521 (2006)
- 4) JH. Lee *et al.*, *Proc. Natl. Acad. Sci. USA*, **102**, 18902 (2005)
- 5) NS. Que-Gewirth *et al.*, Gene therapy progress and prospects: RNA aptamers, in *Gene Ther.*, pp 283 (2007)
- 6) P. Colas *et al.*, *Nature*, **380**, 548 (1996)
- 7) C. Kunz *et al.*, *Mol. Cancer Res.*, **4**, 983 (2006)
- 8) K. Nagel-Wolfrum *et al.*, *Mol. Cancer Res.*, **2**, 170 (2004)
- 9) JM. Polo *et al.*, *Nat. Med.*, **10**, 1329 (2004)
- 10) A. Chattopadhyay *et al.*, *Oncogene*, **25**, 2223 (2006)
- 11) AL. Nouvion *et al.*, *Oncogene*, **26**, 701 (2007)
- 12) E. Tomai *et al.*, *J. Biol. Chem.*, **281**, 21345 (2006)
- 13) JH. Blum *et al.*, *Proc. Natl. Acad. Sci. USA*, **97**, 2241 (2000)
- 14) D. Smith *et al.*, *Chem. Biol.*, **2**, 741 (1995)
- 15) R. Pollock *et al.*, *Nucleic Acids Res.*, **18**, 6197 (1990)
- 16) A. Rhie *et al.*, *J. Biol. Chem.*, **278**, 39697 (2003)
- 17) JC. Cox *et al.*, *Bioorg. Med. Chem.*, **9**, 2525 (2001)
- 18) M. Blank *et al.*, *J. Biol. Chem.*, **276**, 16464 (2001)
- 19) D. Shangguan *et al.*, *Proc. Natl. Acad. Sci. USA*, **103**, 11838 (2006)
- 20) TS. Misono *et al.*, *Anal. Biochem.*, **342**, 312 (2005)
- 21) SD. Mendonsa *et al.*, *J. Am. Chem. Soc.*, **127**, 9382 (2005)
- 22) SD. Mendonsa *et al.*, *Anal. Chem.*, **76**, 5387 (2004)
- 23) M. Berezovsk *et al.*, *J. Am. Chem. Soc.*, **128**, 1410 (2006)
- 24) MB. Bickle *et al.*, *Nat. Protoc.*, **1**, 1066 (2006)
- 25) C. Buerger *et al.*, *J. Cancer Res. Clin. Oncol.*, **129**, 669 (2003)
- 26) RH. Hoess *et al.*, *Chem. Rev.*, **101**, 3205 (2001)
- 27) RC. Ladner *et al.*, *Drug. Discov. Today*, **9**, 525 (2004)
- 28) DN. Krag *et al.*, *Cancer Res.*, **66**, 7724 (2006)
- 29) A. Rothe *et al.*, *FASEB J.*, **20**, 1599 (2006)
- 30) F. Hoppe-Seyler *et al.*, *J. Mol. Med.*, **78**, 426 (2000)
- 31) D. Lipovsek *et al.*, *J. Immunol. Methods*, **290**, 51 (2004)
- 32) X. Yan *et al.*, *Drug. Discov. Today*, **11**, 911 (2006)
- 33) A. Rothe *et al.*, *Expert Opin. Biol. Ther.*, **6**, 177 (2006)
- 34) AD. Keefe *et al.*, *Nature*, **410**, 715 (2001)
- 35) DS. Wilson *et al.*, *Proc. Natl. Acad. Sci. USA*, **98**, 3750 (2001)
- 36) E. Miyamoto-Sato *et al.*, *J. Drug Target.*, **14**, 505 (2006)
- 37) S. Jhaveri *et al.*, *Nat. Biotechnol.*, **18**, 1293 (2000)
- 38) S. Hoshika *et al.*, *FEBS Lett.*, **579**, 3115 (2005)
- 39) J. Chelliserrykatti *et al.*, *Nat. Biotechnol.*, **22**, 1155 (2004)
- 40) PE. Burmeister *et al.*, *Chem. Biol.*, **12**, 25 (2005)
- 41) AD. Frankel *et al.*, *Cell*, **55**, 1189 (1988)

- 42) G. Elliott *et al.*, *Cell*, **88**, 223 (1997)
- 43) B. Gupta *et al.*, *Expert Opin Drug Deliv.*, **3**, 177 (2006)
- 44) S. Futaki, *Biopolymers*, **84**, 241 (2006)
- 45) JS. Wadia *et al.*, *Adv. Drug Deliv. Rev.*, **57**, 579 (2006)
- 46) SM. Nimjee *et al.*, *Mol. Ther.*, **14**, 408 (2006)

# Modification of the titan surface with photoreactive gelatin to regulate cell attachment

Mojgan Heydari,<sup>1</sup> Hirokazu Hasuda,<sup>1</sup> Makoto Sakuragi,<sup>1</sup> Yasuhiro Yoshida,<sup>2</sup>  
Kazuomi Suzuki,<sup>2</sup> Yoshihiro Ito<sup>1,3</sup>

<sup>1</sup>Regenerative Medical Bioreactor Project, Kanagawa Academy of Science and Technology, KSP East 309,  
3-2-1 Sakado, Takatsu-ku, Kawasaki, Kanagawa 213-0012, Japan

<sup>2</sup>Department of Biomaterials, Okayama University Graduate School of Medicine, Dentistry and Pharmaceutical Sciences  
2-5-1 Shikata-cho, Okayama 700-8525, Japan

<sup>3</sup>Nano Medical Engineering Laboratory, RIKEN (The Institute of Physical and Chemical Research),  
2-1 Hirosawa, Wako, Saitama 351-0198, Japan

Received 27 March 2006; revised 7 November 2006; accepted 20 February 2007

Published online 13 June 2007 in Wiley InterScience (www.interscience.wiley.com). DOI: 10.1002/jbm.a.31368

**Abstract:** Titan (TiO<sub>2</sub>) was modified with photoreactive gelatin in order to regulate the attachment of cells. Photoreactive gelatin, which was synthesized by the coupling reaction of gelatin with *N*-(4-azidobenzoyloxy) succinimide, was immobilized onto the *n*-octadecyltrimethoxysilane (ODS)-TiO<sub>2</sub> or TiO<sub>2</sub> surface by ultraviolet irradiation both in the absence and presence of a photo mask. In the absence of a photo mask, the modified titan surface was analyzed by measuring water contact angles and X-ray photoelectron spectroscopy (XPS). The result showed that ODS hydrophobilized the titan surface, and that the immobilization of gelatin affected the surface's hydrophilicity. XPS shows that titan was covered with organic material, including ODS and gelatin. With the photo mask in place,

micropatterning of the gelatin was performed. This pattern was confirmed by optical microscopy and time-of-flight secondary ion-mass spectroscopy (TOF-SIMS). Monkey COS-7 epithelial cells were cultured on the unpattern- and pattern-immobilized plate. A significantly higher degree of cell attachment was found on the photoreactive gelatin-immobilized regions than on those that were not immobilized. It was concluded that the cellular pattern on titan was regulated by immobilized photoreactive gelatin. © 2007 Wiley Periodicals, Inc. *J Biomed Mater Res* 83A: 906–914, 2007

**Key words:** cell adhesion; photoimmobilization; gelatin; titan; micropatterning

## INTRODUCTION

Titanium and titanium alloy implants are widely used in medicine because of their biocompatibility, nontoxicity, good mechanical properties, and excellent corrosion resistance. The surface properties of these materials are of prime importance in establishing the required tissue response, with topography appearing to provide a set of very powerful signals for cells. The chemical surface properties of titanium metal on exposure to air are determined by the properties of an oxide layer (TiO<sub>2</sub>), a few nanometers thick, which passivates the metal. Therefore, the present investigators sought methods whereby this biomaterial might be modified in order to induce biological activity on its surface.<sup>1</sup>

Covalent immobilization of biological molecules onto titan has been performed by several researchers in order to induce specific biological responses. Endo<sup>2,3</sup> employed a chemical modification technique for metal surfaces, which had previously been applied to biosensors for the covalent immobilization of biofunctional proteins on a metallic implant with a surface of nickel–titanium (NiTi) alloy. First,  $\gamma$ -aminopropyltriethoxysilane (APS) was applied to the NiTi substrate to introduce amino groups onto it. Subsequently, human plasma fibronectin was covalently immobilized through Schiff's base formation to enhance the attachment and spreading of cells. Nanci et al.<sup>4</sup> also immobilized either alkaline phosphatase or albumin onto titan by the same method. On the other hand, Xiao et al.<sup>5</sup> used APS for surface modification, and a heterobifunctional cross linker, *N*-succinimidyl-3-maleimidopropionate, reacted with the terminal amino groups to form the exposed maleimide groups. Finally, a model cell-binding peptide, Arg-Gly-Asp-Cys, was immobilized on the surface

Correspondence to: Y. Ito; e-mail: y-ito@riken.jp

through the covalent addition of cysteine thiol groups to the maleimide groups. Similarly, Porte-Durrieu et al.<sup>6</sup> modified Ti-6Al-4V alloy with linear RGD and cyclo-DfKRG.

Weber et al.<sup>7</sup> synthesized 1-aziglycoses, which is a glucose-containing diazirine. Because of the low pKa value and the expected weak nucleophilicity of the hydroxyl groups on the surface of oxidized titanium, 1-aziglycoses modified the titan. The chemicals generated singlet carbenes that were readily inserted into H—O bonds, leading to the glycosidation of titan. Mikulec and Puleo<sup>8</sup> used *p*-nitrophenyl chloroformate to immobilize trypsin on Ti-6Al-4V. Puleo et al.<sup>9</sup> also modified a plasma surface through the polymerization of allylamine in order to enable the immobilization of bioactive molecules on Ti-6Al-4V, a "bioinert" metal. Bone morphogenetic protein 4 (BMP-4) was immobilized on the aminated surface by carbodiimide. These investigators reported that the resulting BMP-4-bound surface induced alkaline phosphatase activity in pluripotent C3H10T1/2 cells.

In addition to covalent modification, some studies of noncovalent modification have also been done by several researchers. Barber et al.<sup>10</sup> grafted peptide-modified p(AAm-co-EG/AAC) IPN to titanium, the surface of which then supported the attachment and spreading of primary rat calvarial osteoblasts. Tosatti et al.<sup>11,12</sup> and Hansson et al.<sup>13</sup> synthesized RGD-containing poly(L-lysine)-graft-poly(ethylene glycol) and used it to modify the surface of titanium. Cai et al.<sup>14</sup> improved the surface biocompatibility of titanium films using a layer-by-layer self-assembly technique that was based on the polyelectrolyte-mediated electrostatic adsorption of chitosan and gelatin. The film's growth was initialized by the deposition of one layer of positively charged poly(ethylene imine). Then, utilizing electrostatic interactions, a thin film was formed by the alternate deposition of negatively charged gelatin and positively charged chitosan. Surface modification by protein adsorption has also been reported by several researchers.<sup>15-17</sup>

Thus far, we have modified various polymeric materials with biological molecules by photoimmobilization.<sup>18-26</sup> By this method, pattern immobilization was easily performed. In the present study, photo-reactive gelatin was used for the surface modification of titan. The surface property was characterized and a micropatterned surface was prepared by using a photo mask. The COS-7 monkey epithelial cells were cultured on the pattern-immobilized plate, after which the cell behavior was observed. To easily observe the cells by optical microscopy, the immobilization of gelatin was performed on thin titanium-coated glass plate. This represents the first report of the surface patterning of TiO<sub>2</sub> with biological molecules. The micropatterning of surface was considered to be useful to clarify the immobilization and to

compare the effect of immobilized and nonimmobilized regions. In addition, surface patterning technique is expected to develop some new medical applications of titanium.

## MATERIALS AND METHODS

### Materials

*N,N*-Dimethylformamide (DMF), paraformaldehyde, 1,4-dioxane (diethylene dioxide), and dehydrated toluene were purchased from Wako Pure Chemicals (Osaka, Japan). Dicyclohexylcarbodiimide (DCC) and 4-azidobenzoic acid were purchased from Tokyo Kasei (Tokyo, Japan). *N*-Hydroxysuccinimide was purchased from Protein Institute (Minoh, Japan). Gelatin was purchased from Becton Dickinson (Maryland, USA). *n*-Octadecyltrimethoxysilane [ODS, CH<sub>3</sub>(CH<sub>2</sub>)<sub>17</sub>Si(OCH<sub>3</sub>)<sub>3</sub>] was purchased from ShinEtsu (Tokyo, Japan). Glutaraldehyde 25% was purchased from Polysciences (Warrington, PA). COS-7, the monkey kidney epithelial-like cell line, was provided by RIKEN Cell Bank (Tsukuba, Japan) and maintained in Dulbecco modified Eagle's medium (DMEM) (Sigma, St. Louis, MO) supplemented with 10% fetal bovine serum (FBS) (Moregate, Australia and New Zealand). Trypsin (2.5%) was purchased from Invitrogen (New York). Ethylenediaminetetraacetic acid (EDTA) was purchased from Dojindo (Kumamoto, Japan).

A glass plate (15 mm in diameter and 1 mm thick) was coated with titanium by Osaka Vacuum Ind. (Osaka, Japan). This plate was then cleaned by ultrasonication in ultrapure water nine times and dried with heated gas. Pure titanium was vacuum-deposited on the plate by an electron beam 400 nm ( $\pm 25\%$ ) wide. The thickness of titanium layer was controlled to keep the transparency for optically microscopic observation. Polystyrene plates for tissue culture, each with 24 wells (well diameter 16 mm), were purchased from Asahi Techno Glass (Chiba, Japan).

### Surface treatment with ODS

The surfaces of the titan plates were photochemically cleaned by an excimer ultraviolet (UV) lamp (USHIO, Tokyo, Japan) for 10 min. This method was applied for the complete removal of C—C bonds and subsequent decomposition of the organic molecules.<sup>27</sup> Complete removal of the organic material was confirmed by a water contact angle measurement of nearly zero, which is indicative of an absolutely hydrophilic surface.

After this, silane-coupling reaction was performed as follows: The cleaned plates were placed in a flask containing 40 mL of *n*-octadecyltrimethoxysilane (10 mM ODS in dehydrated toluene). The coupling reaction was carried out at 60°C for 5 h. The hydrophobilized plates were rinsed in fresh toluene, followed by drying in a clean vacuum oven at 60°C for 4 h.

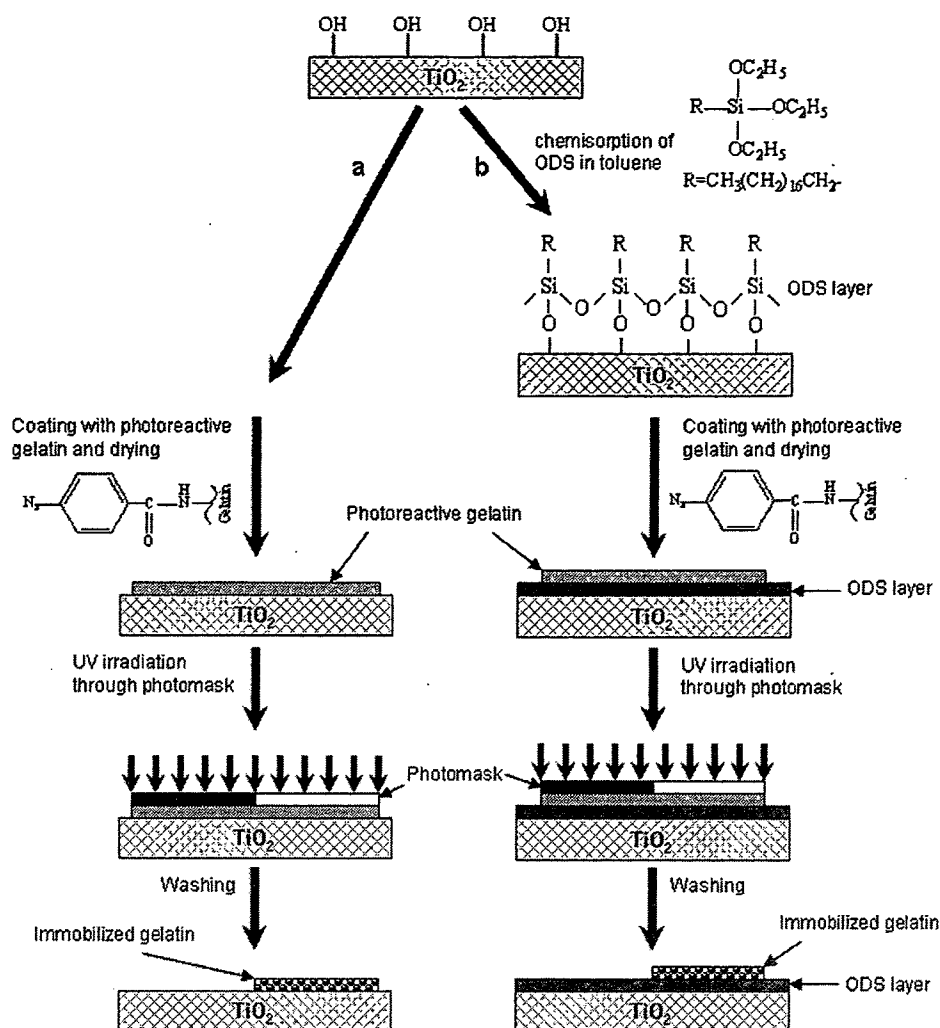


**Figure 1.** Schematic illustration of the pattern-immobilization of photoreactive gelatin on (a) titan and (b) titan modified with ODS.

### Photoreactive gelatin

Photoreactive gelatin was synthesized according to the method previously reported.<sup>28</sup> *N*-(4-Azidobenzoyloxy) succinimide carrying azidophenyl groups was synthesized, as reported by Sugawara and Matsuda.<sup>29</sup> Then 4-azidobenzoic acid (0.018 mM), *N*-hydroxysuccinimide (0.018 mM), and DCC (0.018 mM) were dissolved in 1,4-dioxane (100 mL) and stirred overnight (20 h) in the dark at room temperature. Subsequently, this mixture was concentrated under reduced pressure and crystallized to produce the photoreactive crystal [*N*-(4-azidobenzoyloxy) succinimide] with a yield of about 40%. Afterwards, the gelatin solution in deionized water (33.33 mg/mL) and the photoreactive crystal solution in DMF (10.83 mg/mL) were mixed and stirred overnight in the dark at room temperature. The resulting solution was dialyzed using a seamless cellulose tube (cutoff molecular weight of 10,000). The dialyzed photoreactive gelatin was finally freeze-dried under vacuum to obtain a white solid (yield ~40%), which is used in this

study as the photoreactive gelatin. The content of azidoaniline by UV absorbance as previously reported<sup>28</sup> was 4.45%.

### Measurement of water contact angle

Static water contact angles of the sample surfaces were measured at 25°C in air using a contact angle meter (Kyowa Interface Science, Tokyo, Japan) based on the sessile drop method. All the contact angles were determined by averaging nine different points values measured on each sample surface. An unpatterned plate was used for the contact angle measurements.

### Pattern immobilization of photoreactive gelatin

The procedure of pattern immobilization of photoreactive gelatin is shown in Figure 1. An aqueous solution of photoreactive gelatin (1 mg/mL) was cast onto the surface

of ODS-TiO<sub>2</sub> or TiO<sub>2</sub> and air-dried at room temperature. Subsequently, the plates were covered with and without patterned photo masks and UV irradiated for 10 s using a UV lamp (Hamamatsu Photonics, Shizuoka, Japan) at a distance of 5 cm. The photo mask consisted of a 2-mm-thick quartz glass plate with 93% transparency at 172 nm, and a 0.1- $\mu$ m-thick chromium pattern. The plates were washed thoroughly with cold distilled water.

### TOF-SIMS, XPS, and AFM measurements

Measurement of time-of-flight secondary ion mass spectrometry (TOF-SIMS) was performed using a TFS-2000 (Physical Electronics). The primary ion was <sup>69</sup>Ga<sup>+</sup>; accelerating voltage of the ion gun, 25 kV; pulse width, 12 ns; pulse frequency, 8.3 kHz; range of mass, 0–1000 amu; resolution of time, 1.1 ns/ch.

The surfaces were also analyzed using X-ray photoelectron spectroscopy (XPS) (AXIS-HS, Kratos, Manchester, UK) *in vacuo* of less than 10<sup>-7</sup> Pa. An Al K $\alpha$  monochromatic X-ray with a source power of 150 W was utilized. Wide and narrow scans were measured at pass energy of 80 and 40 eV, respectively. Overview spectra were obtained in the range of 0–1100 eV with analyzer pass energy of 80 and 40 eV. For the XPS measurement, unpatterned plates were employed.

Atomic force microscopic observation was performed using an Nanoscope IV (Digital Instruments). The measurement was performed using the tapping mode with a nominal force constant of 0.09 N/m.

### Cell culture

COS-7 cells were cultured in DMEM supplemented with 10% FBS at 37°C in 95% humidified air and 5% CO<sub>2</sub>. The cells were then washed using 10 mL of phosphate-buffered saline and harvested with a 0.25% trypsin containing 1 mM EDTA solution for 3 min at 37°C. Finally, the recovered cells were suspended in the medium for the *in vitro* examination to follow. The cell suspension was added to 24-well polystyrene plates for tissue culture (1.0 mL per well, 10  $\times$  10<sup>4</sup> cells per milliliter) of which each well contained the sample plates, which had been disinfected with 70% ethanol, washed with sterilized H<sub>2</sub>O, and fixed with a silicon ring. The cells were cultured in a 5% CO<sub>2</sub> atmosphere at 37°C overnight and studied with a phase-contrast microscope. The cell numbers were counted under the microscope. The percentage of adhering cells, calculated from the added suspension of cells, was 100%.

## RESULTS AND DISCUSSION

### Measurement of the water contact angle

Surface hydrophilicity was determined by measuring the contact angle (Fig. 2). The surface of titan was very hydrophilic when the contact angle was measured immediately after cleaning with eximer

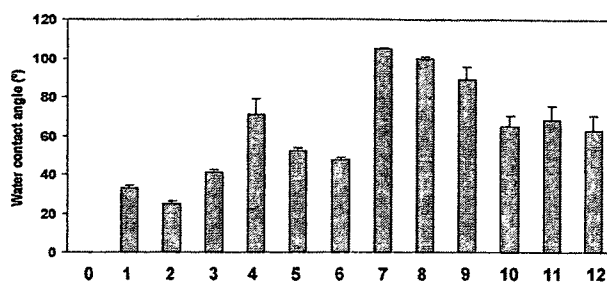


**Figure 2.** Water contact angle measurements of TiO<sub>2</sub>-modified surfaces. (0) TiO<sub>2</sub> photochemically cleaned by an eximer UV lamp, (1) TiO<sub>2</sub> after exposure to air for more than 3 h but before UV irradiation employed for immobilization, (2) TiO<sub>2</sub> after UV irradiation for immobilization, (3) TiO<sub>2</sub>-photoreactive gelatin before UV irradiation for immobilization, (4) TiO<sub>2</sub>-photoreactive gelatin after UV irradiation for immobilization, (5) TiO<sub>2</sub>-unmodified gelatin before UV irradiation for immobilization, (6) TiO<sub>2</sub>-unmodified gelatin after UV irradiation for immobilization, (7) TiO<sub>2</sub>-ODS before UV irradiation for immobilization, (8) TiO<sub>2</sub>-ODS after UV irradiation for immobilization, (9) TiO<sub>2</sub>-ODS-photoreactive gelatin before UV irradiation for immobilization, (10) TiO<sub>2</sub>-ODS-photoreactive gelatin after UV irradiation for immobilization, (11) TiO<sub>2</sub>-ODS-unmodified gelatin before UV irradiation for immobilization, and (12) TiO<sub>2</sub>-ODS-unmodified gelatin after UV irradiation for immobilization. *n* = 10. [Color figure can be viewed in the online issue, which is available at [www.interscience.wiley.com](http://www.interscience.wiley.com).]

UV light (column 0 of Fig. 2). However, the hydrophilic surface was not stable and after exposure to air the surface gradually became hydrophobic (column 1 of Fig. 2). For further experiments, those titan surfaces that had been sufficiently exposed to air and had stable contact angles were employed.

These surfaces were UV irradiated in both the presence and the absence of unmodified or photoreactive gelatin. Gelatin treatment increased the surfaces' hydrophobicity. When the titan surface was coated with photoreactive gelatin and UV irradiated, it proved to be the most hydrophobic (column 4 of Fig. 2). In addition, from comparisons before and after UV irradiation, the most significant difference in hydrophilicity was observed with the titan surface (columns 3 and 4 of Fig. 2). These results indicate that the surface was affected by immobilized gelatin.

It is known that aryl azide derivatives form short-lived nitrenes that react extremely rapidly with their surrounding chemical environment.<sup>30</sup> Recent evidence, however, indicates that the photolyzed intermediates of aryl azides can undergo ring expansion to create nucleophile-reactive dehydroazepines.<sup>31</sup> Earlier, glycosidation of the bare titanium surface using 1-aziglycose had been reported.<sup>7</sup> In the present study, although no chemical evidence that demonstrated the formation of a covalent bond between the hydroxyl groups of titan and the photolyzed groups is presented, the fact that photolyzation induced the

immobilization of gelatin as indicated by the micropatterned immobilization means that immobilization occurred in the region photoirradiated, as shown in following section. It was demonstrated that the same micropattern was formed on the titan in the presence of a photomask and this type of pattern formation was not observed when unmodified gelatin was employed. It is difficult to conclude that the immobilization was due to covalent bonding. Some anchoring effect onto the titan was also taken into consideration. However, gelatin immobilization on titan was strongly suggested by the micropatterning.

On the other hand, the water contact angle increased with ODS treatment (columns 7–12 of Fig. 2). In these cases, hydrophobicity decreased with gelatin immobilization. In particular, photoreactive gelatin had the most significant effect on surfaces (columns 8 and 10 of Fig. 2). This demonstrates that upon UV irradiation, the generated radical groups bonded together with neighboring hydrocarbons in the ODS-treated  $\text{TiO}_2$  plate surface, as previously reported for organic materials.

The  $\text{TiO}_2$  surfaces treated with photoreactive gelatin (column 4 of Fig. 2) and  $\text{TiO}_2$ -ODS treated with photoreactive gelatin (column 10 of Fig. 2) had almost the same water contact angles. This indicates that the surfaces were almost completely covered with photoreactive gelatin and showed the same hydrophilicity. On the other hand, the effect of unmodified gelatin was the same before and after UV irradiation, considering that it neither hydrophobilized  $\text{TiO}_2$  (columns 5 and 6 of Fig. 2) very much, nor hydrophilized ODS-treated  $\text{TiO}_2$  (columns 11 and 12 of Fig. 2). We considered that a sufficient quantity of unmodified gelatin could not be adsorbed onto the  $\text{TiO}_2$  surface.

#### TOF-SIMS, XPS, and AFM analysis of the $\text{TiO}_2$ surfaces

To evaluate  $\text{TiO}_2$ -ODS surfaces, XPS analysis was carried out on  $\text{TiO}_2$ -ODS treated with photoreactive gelatin before and after UV irradiation (Fig. 3). Peaks of Ti were detected in ODS-treated  $\text{TiO}_2$  [Fig. 3(a)]. After photoreactive gelatin immobilization onto the ODS-treated  $\text{TiO}_2$ , a  $\text{N}_{1s}$  peak appeared, indicating the presence of nitrogen in the gelatin [Fig. 3(b)]. The same phenomenon was observed on  $\text{TiO}_2$  modification. However, it was very difficult to observe the gelatin bond with the titan surface by XPS analysis. Considering that the concentration of photoreactive groups is very low and the bond will be formed only on the interface, it is very hard to detect the bond. Therefore, micropatterning was performed. If the micropattern was formed, we considered that photoimmobilization had occurred.

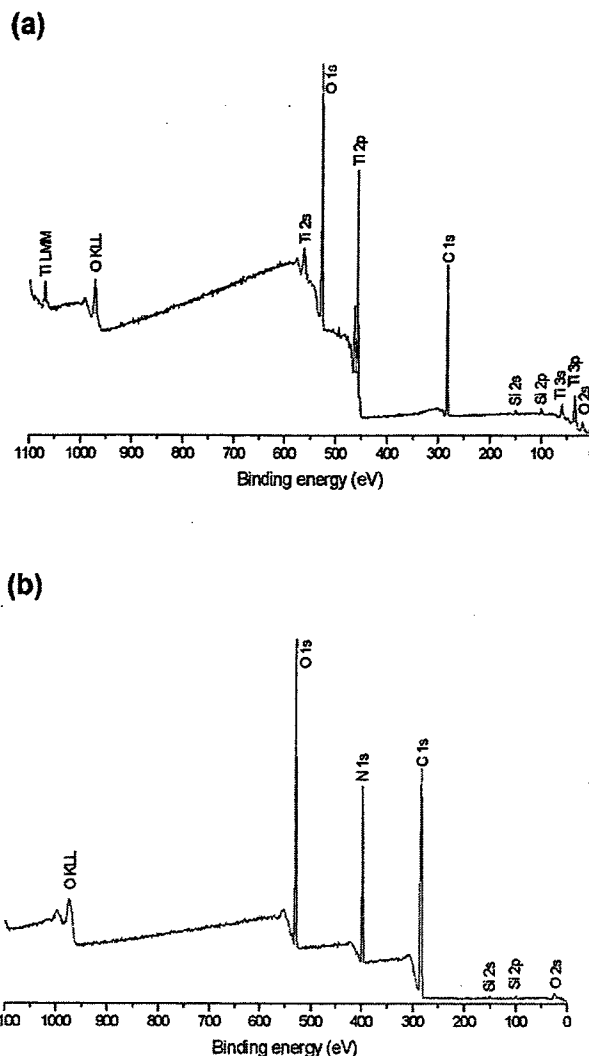


**Figure 3.** XPS wide scan spectrum of titanium treated (a) with ODS and (b) with photoreactive gelatin.

The micropatterned surface was first observed by phase-contrast microscopy (Fig. 4). The same micropattern was formed on modified titan in the presence of a photo mask. This type of pattern formation was not observed when unmodified gelatin was employed. In addition, the surface was measured by TOF-SIMS. Secondary ion images obtained by TOF-SIMS analysis of the secondary positively and negatively charged ions of the micropatterned surface are shown in Figure 5. In the positively charged ion image [Fig. 5(b)], a high density of  $^{48}\text{Ti}^+$  was observed on the nonimmobilized regions. However, on the regions immobilized with gelatin, organic materials in high density were observed in the negatively charged ion image [Fig. 5(c)].

To observe the thickness of immobilized gelatin, the surface was observed by AFM (Fig. 6). The thickness of immobilized gelatin was about 300 nm on both bare and ODS-treated titans.

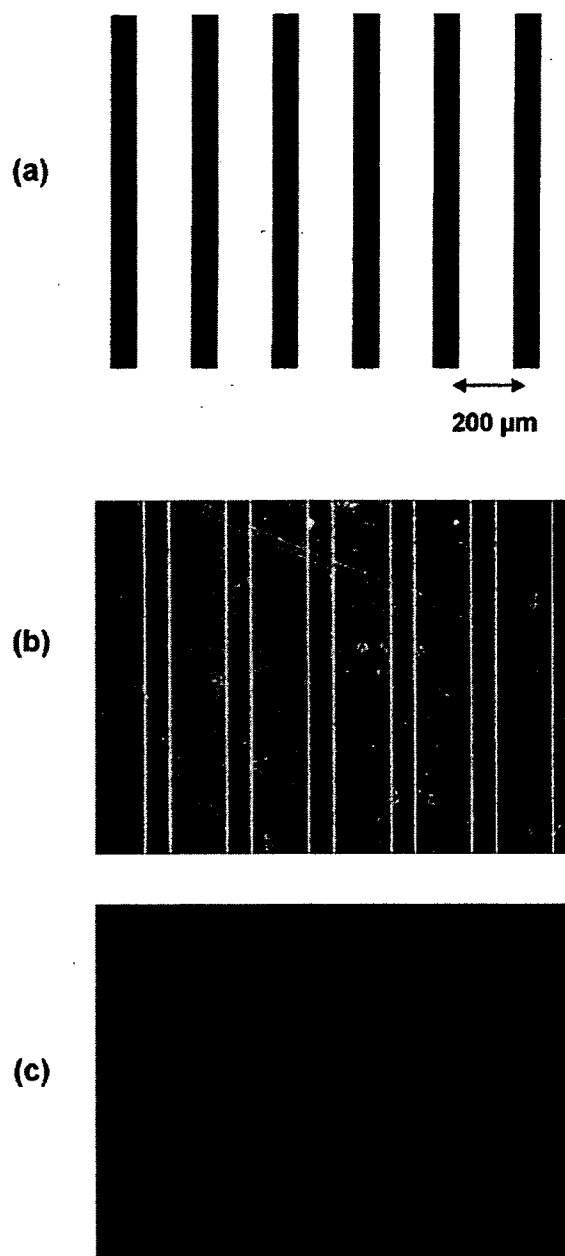


**Figure 4.** Optical microscopic micrographs of (a) photomask and immobilized pattern of photoreactive gelatin in a striped pattern on (b)  $\text{TiO}_2$  and (c)  $\text{TiO}_2\text{-ODS}$ . [Color figure can be viewed in the online issue, which is available at [www.interscience.wiley.com](http://www.interscience.wiley.com).]

#### Cell adhesion on modified surfaces

Figure 7 shows the result of adhered COS-7 cells on the modified titan surfaces. When the surface of titan was immediately cleaned with excimer light, cell attachment was enhanced (column 0 of Fig. 7). However, attachment was enhanced to a lesser degree on the surface exposed to air for a considerable time (column 1 of Fig. 7). The cleaned titan sur-

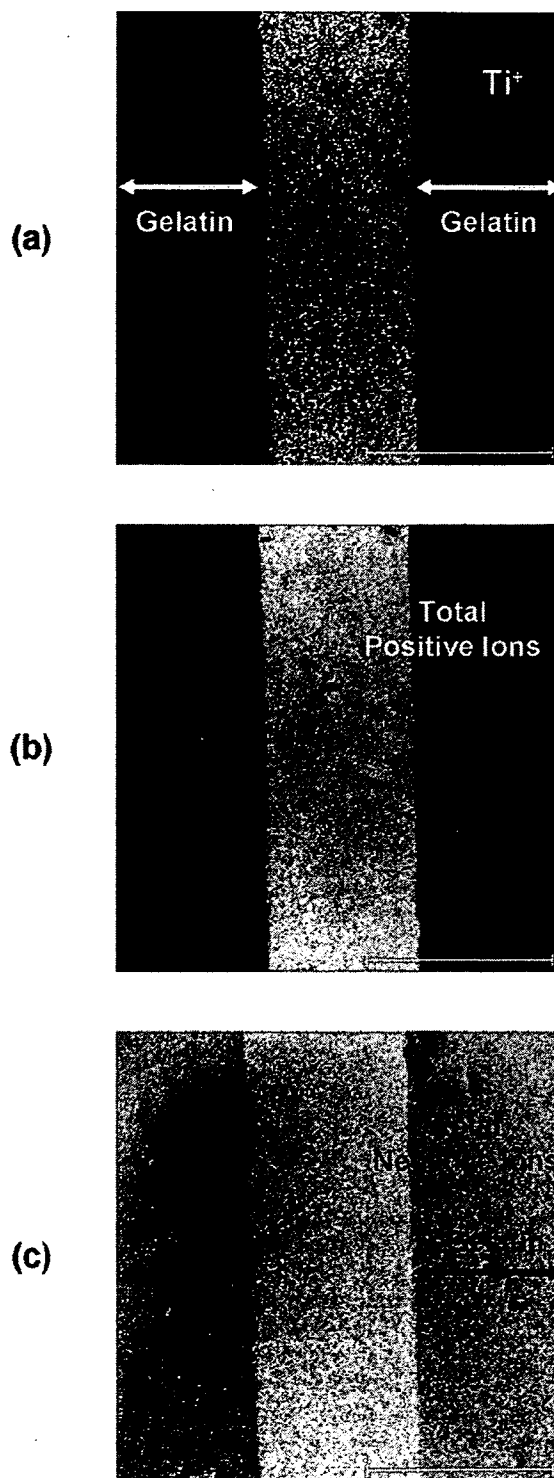


**Figure 5.** TOF-SIMS images of micropattern-immobilized titan surface. (a) The secondary positively charged total ions, (b) titanium ion, and (c) secondary negatively charged total ions. Length scale: 100  $\mu\text{m}$ , 600.2 s using LMIG - ions (240.0  $\times$  240.0  $\mu\text{m}$ ). [Color figure can be viewed in the online issue, which is available at [www.interscience.wiley.com](http://www.interscience.wiley.com).]

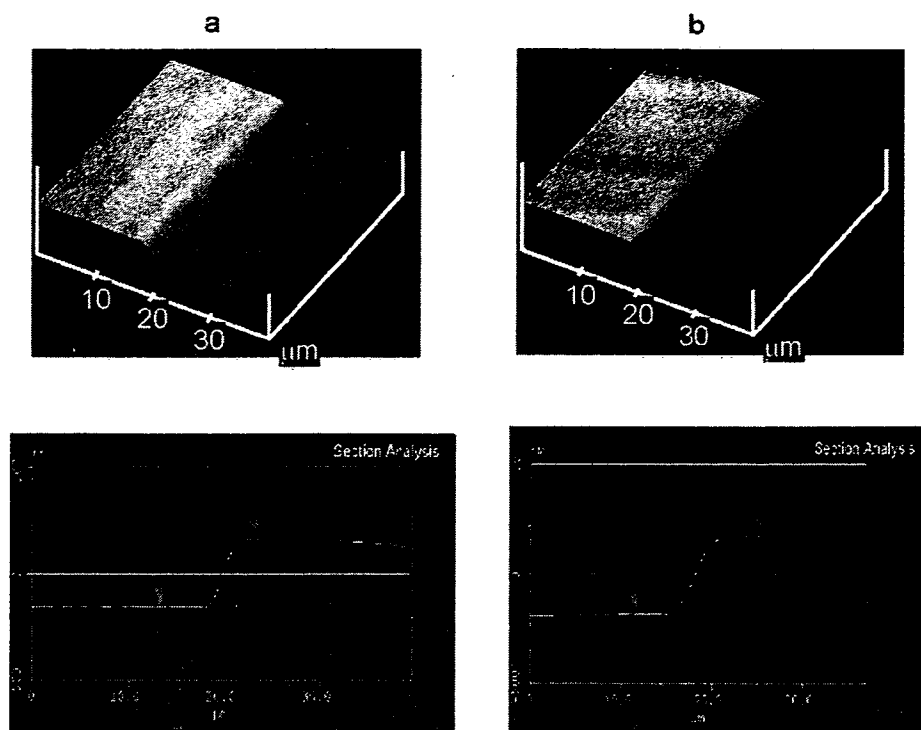


**Figure 6.** AFM images of gelatin layer of micropattern-immobilized on (a)  $\text{TiO}_2$  and (b)  $\text{TiO}_2$ -ODS. The cross sections of AFM images of gelatin layer of micropattern-immobilized on (c)  $\text{TiO}_2$  and (d)  $\text{TiO}_2$ -ODS. [Color figure can be viewed in the online issue, which is available at [www.interscience.wiley.com](http://www.interscience.wiley.com).]

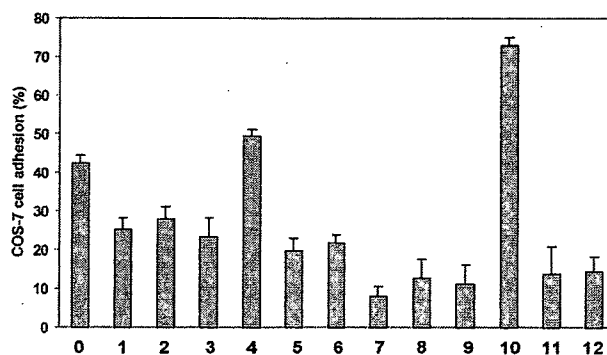
face may have provided some condition for cell attachment independent of hydrophilicity. Photoimmobilized gelatin significantly enhanced cell adhesion, as shown in column 4 of Figure 7.

ODS treatment of the surfaces did not enhance cell attachment. This reduction is believed to be due to hydrophobization. However, photoimmobilized gelatin significantly enhanced cell adhesion (column 10 of Fig. 7). The cells adhered to photoreactive gelatin-immobilized titan twice as well as on normal titan. Although comparison of gelatin-immobilized with nonimmobilized surfaces depended on the property of nonimmobilized surface, enhancement of cell adhesion by gelatin immobilization was not so significantly different (columns 4 and 10 in Fig. 7). Considering that both of the surfaces were covered with gelatin as shown in Figure 6, the same level of enhancement was reasonable.

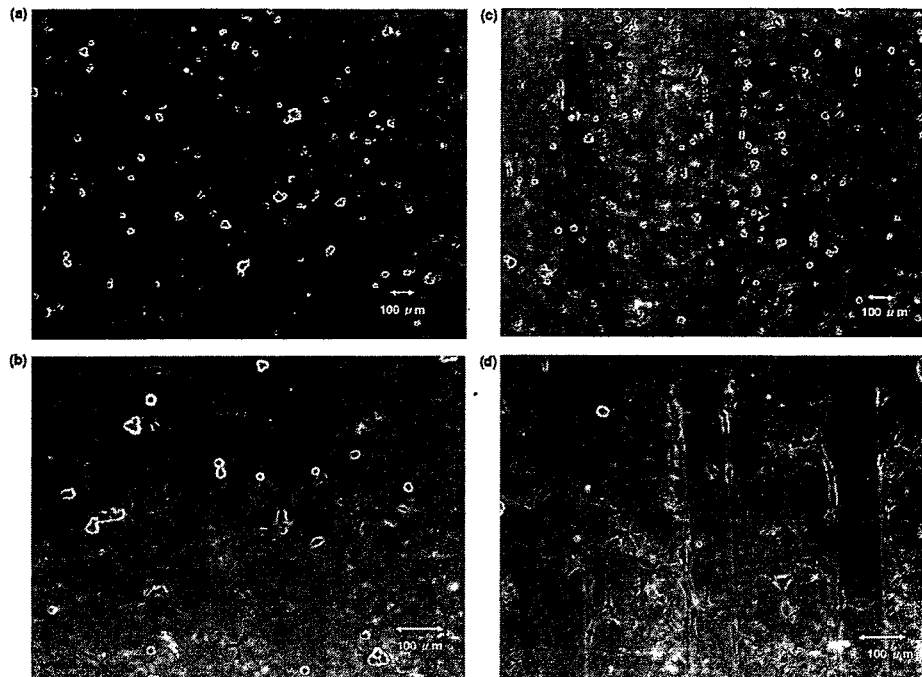
#### Cell adhesion on pattern-immobilized gelatin

Figure 8 shows the adhesion of COS-7 cell on the pattern-immobilized gelatin surfaces of both  $\text{TiO}_2$  and  $\text{TiO}_2$ -ODS. In the case of  $\text{TiO}_2$  surface [Fig. 8(a)], COS-7 cells adhered to immobilized photoreactive gelatin a little more than to titan (1.5 times estimated from the photos) as expected from the comparison between columns 3 and 4 in Figure 7 (2.1 times). On

the other hand, COS-7 cell significantly adhered on the immobilized photoreactive gelatin regions of ODS-modified surfaces [Fig. 8(b)]. Since 6.5 times as many as cells adhered to the photoreactive gelatin-



**Figure 7.** Adhesion of COS-7 cells on different surfaces of (0)  $\text{TiO}_2$ , (1)  $\text{TiO}_2$  before UV irradiation, (2)  $\text{TiO}_2$  after UV irradiation, (3)  $\text{TiO}_2$ -photoreactive gelatin before UV irradiation, (4)  $\text{TiO}_2$ -photoreactive gelatin after UV irradiation, (5)  $\text{TiO}_2$ -unmodified gelatin before UV irradiation, (6)  $\text{TiO}_2$ -unmodified gelatin after UV irradiation, (7)  $\text{TiO}_2$ -ODS before UV irradiation, (8)  $\text{TiO}_2$ -ODS after UV irradiation, (9)  $\text{TiO}_2$ -ODS-photoreactive gelatin before UV irradiation, (10)  $\text{TiO}_2$ -ODS-photoreactive gelatin after UV irradiation, (11)  $\text{TiO}_2$ -ODS-unmodified gelatin before UV irradiation, and (12)  $\text{TiO}_2$ -ODS-photoreactive gelatin after UV irradiation.  $n = 10$ . [Color figure can be viewed in the online issue, which is available at [www.interscience.wiley.com](http://www.interscience.wiley.com).]



**Figure 8.** Adhesion of COS-7 cells on photoreactive gelatin micropattern-immobilized (a,b)  $\text{TiO}_2$  and (c,d)  $\text{TiO}_2$ -ODS. [Color figure can be viewed in the online issue, which is available at [www.interscience.wiley.com](http://www.interscience.wiley.com).]

immobilized surface as to the ODS-modified surface (columns 9 and 10 in Fig. 7), the pattern of cell adhesion was very clear (7.6 times estimated from the photos). These results demonstrate that the cell adhesion behavior on micropatterned surface (Fig. 8) is similar to that on homogeneous surfaces (Fig. 7). Moreover, the difference between nonimmobilized and immobilized regions was enhanced with increasing cell culture time.

The morphology change is estimated by the ratio of spread cells over round-shaped cells on immobilized and nonimmobilized regions. On  $\text{TiO}_2$  spread cells ratio on gelatin-immobilized regions was 2.1 times as many as that on nonimmobilized regions and on ODS-treated  $\text{TiO}_2$  the ratio was 6.6 times, according to the photos in Figures 8(b) and 8(d), respectively. Considering these ratios corresponded to the number of adhered cells, the spreading increased with the increase of adhesiveness.

## CONCLUSION

The photoimmobilization of biological molecules on titanium surfaces was performed, and micropattern immobilization on the titan surface was achieved. The patterning of metal surfaces in this manner will be useful for medical and biotechnological applications.

This study was supported in part by a Grant-in-aid for Scientific Research (No. 18390513) from the Ministry of Education, Culture, Sports, Science, and Technology of Japan (2006–2008).

## References

1. Xiao SJ, Kenausis G, Textor M. Biochemical modifications of titanium surface. In: Brunette DM, Tengvall P, Textor M, Thomsen P, editors. *Titanium in Medicine*. Springer, Berlin; 2001. p 417–455.
2. Endo K. Chemical modification of metallic implant surfaces with biofunctional proteins, Part 1: Molecular structure and biological activity of a modified alloy surface. *Dent Mater J* 1995;14:185–198.
3. Endo K. Chemical modification of metallic implant surfaces with biofunctional proteins, Part 2: Corrosion resistance of a chemically modified NiTi alloy. *Dent Mater J* 1995;14:199–210.
4. Nanci A, Wuest JD, Peru L, Brunet P, Sharma V, Zalzal S, McKee MD. Chemical modification of titanium surfaces for covalent attachment of biological molecules. *J Biomed Mater Res* 1998;40:324–335.
5. Xiao SJ, Textor M, Spencer ND, Wieland M, Keller B, Sigrist H. Immobilization of the cell-adhesive peptide Arg-Gly-Asp-Cys (RGDC) on titanium surfaces by covalent chemical attachment. *J Mater Sci Mater Med* 1997;8:867–872.
6. Porte-Durrieu MC, Guillemot F, Pallu S, Labrugere C, Brouilaud B, Bareille R, Amedee J, Barthe N, Dard M, Baquey Ch. Cyclo-(DfKRG) peptide grafting onto Ti-6Al-4V: Physical characterization and interest towards human osteoprogenitor cells adhesion. *Biomaterials* 2004;25:4837–4846.
7. Weber M, Vasella A, Textor M, Spencer M. Glucosidation of titanium dioxide with 1-aziglucoses: Preparation and characterization of modified titanium-oxide surfaces. *Helv Chim Acta* 1998;81:1359–1372.

8. Mikulec LJ, Puleo DA. Use of *p*-nitrophenyl chloroformate chemistry to immobilize protein on orthopedic biomaterials. *J Biomed Mater Res* 1996;32:203–208.
9. Puleo DA, Kissling RA, Sheu MS. A technique to immobilize bioactive proteins, including bone morphogenetic protein-4 (BMP-4), on titanium alloy. *Biomaterials* 2002;23:2079–2087.
10. Barber TA, Golledge SL, Castner DG, Healy KE. Peptide-modified p(AAm-co-EG/AAc) IPNs grafted to bulk titanium modulate osteoblast behavior in vitro. *J Biomed Mater Res A* 2003;64:38–47.
11. Tosatti S, De Paul SM, Askendal A, VandeVondele S, Hubbell JA, Tengvall P, Textor M. Peptide functionalized poly(L-lysine)-*g*-poly(ethylene glycol) on titanium: Resistance to protein adsorption in full heparinized human blood plasma. *Biomaterials* 2003;24:4949–4958.
12. Tosatti S, Schwartz Z, Campbell C, Cochran DL, VandeVondele S, Hubbell JA, Denzer A, Simpson J, Wieland M, Lohmann CH, Textor M, Boyan BD. RGD-containing peptide GCRGYGRGDSPPG reduces enhancement of osteoblast differentiation by poly(L-lysine)-*graft*-poly(ethylene glycol)-coated titanium surfaces. *J Biomed Mater Res A* 2004;68:458–472.
13. Hansson KM, Tosatti S, Isaksson J, Wettero J, Textor M, Lindahl TL, Tengvall P. Whole blood coagulation on protein adsorption-resistant PEG and peptide functionalised PEG-coated titanium surfaces. *Biomaterials* 2005;26:861–872.
14. Cai K, Rechtenbach A, Hao J, Bossert J, Jandt KD. Polysaccharide-protein surface modification of titanium via a layer-by-layer technique: Characterization and cell behaviour aspects. *Biomaterials* 2005;26:5960–5971.
15. Morra M, Cassinelli C, Cascardo G, Cahalan P, Cahalan L, Fini M, Giardino R. Surface engineering of titanium by collagen immobilization. Surface characterization and in vitro and in vivo studies. *Biomaterials* 2003;24:4639–4654.
16. Park BS, Heo SJ, Kim CS, Oh JE, Kim JM, Lee G, Park WH, Chung CP, Min BM. Effects of adhesion molecules on the behavior of osteoblast-like cells and normal human fibroblasts on different titanium surfaces. *J Biomed Mater Res A* 2005;74:640–651.
17. Ku Y, Chung CP, Jang JH. The effect of the surface modification of titanium using a recombinant fragment of fibronectin and vitronectin on cell behavior. *Biomaterials* 2005;26:5153–5157.
18. Ito Y, Kondo S, Chen G, Imanishi Y. Patterned artificial stimulation of cells by covalently immobilized insulin. *FEBS Lett* 1997;403:159–162.
19. Ito Y, Hayashi M, Imanishi Y. Gradient micropattern immobilization of heparin and its interaction with cells. *J Biomater Sci Polym Ed* 2001;12:367–378.
20. Ito Y, Chen G, Imanishi Y. Micropatterned immobilization of epidermal growth factor to regulate cell function. *Bioconjug Chem* 1998;9:277–282.
21. Ito Y, Chen G, Imanishi Y. Artificial juxtacrine stimulation for tissue engineering. *J Biomater Sci Polym Ed* 1998;9:879–890.
22. Ito Y, Chen G, Imanishi Y. Photoimmobilization of insulin onto polystyrene dishes for protein-free cell culture. *Biotechnol Prog* 1996;12:700–702.
23. Chen G, Ito Y, Imanishi Y, Magnani A, Lamponi S, Barbucci R. Photoimmobilization of sulfated hyaluronic acid for anti-thrombogenicity. *Bioconjug Chem* 1997;8:730–734.
24. Chen G, Ito Y, Imanishi Y. Photo-immobilization of epidermal growth factor enhances its mitogenic effect by artificial juxtacrine signaling. *Biochim Biophys Acta* 1997;1358:200–208.
25. Ito Y. Surface micropatterning to regulate cell functions. *Biomaterials* 1999;20:2333–2342.
26. Ito Y, Li JS, Takahashi T, Imanishi Y, Okabayashi Y, Kido Y, Kasuga M. Enhancement of the mitogenic effect by artificial juxtacrine stimulation using immobilized EGF. *J Biochem* 1997;121:514–520.
27. Sugimura H, Ushiyama K, Hozumi A, Takai O. Micropatterning of alkyl- and fluoroalkylsilane self-assembled monolayers using vacuum ultraviolet light. *Langmuir* 2000;16:885–888.
28. Ito Y, Hasuda H, Yamauchi T, Komatsu N, Ikebuchi K. Immobilization of erythropoietin to culture erythropoietin-dependent human leukemia cell line. *Biomaterials* 2004;25:2293–2298.
29. Matsuda T, Sugawara T. Photochemical protein fixation on polymer surfaces via derivatized phenyl azido group. *Langmuir* 1995;11:2272–2276.
30. Gilchrist TL, Rees CW. Carbenes, Nitrenes, and Arynes (Studies in Modern Chemistry). London: Nelson; 1969. p 131.
31. Hermanson GH. *Bioconjugate Techniques*. San Diego: Academic Press; 1996. p 255.

## Copolymers Including L-Histidine and Hydrophobic Moiety for Preparation of Nonbiofouling Surface

Takehiko Ishii,<sup>†,||</sup> Akira Wada,<sup>†</sup> Saki Tsuzuki,<sup>‡</sup> Mario Casolaro,<sup>§</sup> and Yoshihiro Ito<sup>\*,†,‡</sup>

Nano Medical Engineering Laboratory, RIKEN (The Institute of Physical and Chemical Research), 2-1 Hirosawa, Wako, Saitama, 351-0198, Japan, Regenerative Medical Bioreactor Project, Kanagawa Academy of Science and Technology, KSP East 309, 3-2-1 Sakado, Takatsu-ku, Kawasaki, Kanagawa, 213-0012, Japan, and Dipartimento di Scienze e Tecnologie Chimiche e dei Biosistemi, Università degli Studi di Siena, Via Aldo Moro 2, 1-53100 Siena, Italy

Received April 18, 2007; Revised Manuscript Received July 26, 2007

A new type of copolymer composed of L-histidine (ampholyte) and *n*-butyl methacrylate (hydrophobic moiety) was developed for the preparation of nonbiofouling surfaces. The copolymer adsorbed onto resin surfaces and made the surface very hydrophilic. The hydrophilization effect was higher than that of bovine serum albumin (BSA). When polystyrene surfaces were coated with the copolymer, both the nonspecific adsorption of protein and the adhesion of cells were significantly reduced in comparison with BSA coating. The newly synthesized polymer is a new and useful candidate for the preparation of nonbiofouling surfaces.

### Introduction

The preparation of nonfouling surfaces that prevent nonspecific adsorption of proteins and adhesion of cells is important in the development of therapeutic and diagnostic devices. Typically, surface modification with polyethylene glycol (PEG), PEGylation, has been performed for this purpose.<sup>1</sup> PEG is a nontoxic, nonimmunogenic, uncharged polymer that is soluble in water. The hydrophilicity, high mobility, large excluded volume, and steric hindrance effects of PEG contributed to surface-immobilized PEGs ability to resist cell adhesion and protein adsorption.<sup>2–4</sup>

In addition, biomimetic approaches using cell-surface-mimicking polymers have been investigated. One approach is to design interface materials based on the cell surface glycocalyx, which is a complex coating of highly glycosylated molecules that dominate the interface between a cell and its environment.<sup>5,6</sup> Another approach is based on cell surface lipids.<sup>7–18</sup> Nakabayashi and Ishihara have developed a useful polymer using this mimicking method.<sup>7–12</sup> They prepared a phospholipid polymer with a 2-methacryloyloxyethyl phosphatidylcholine (MPC) moiety and demonstrated that the polymer adsorbed onto materials surfaces to reduce interaction with various types of proteins and cells. Kitano et al.<sup>19,20</sup> reported that water-soluble neutral polymers do not disturb the structure of water significantly, whereas the electrostriction effect of polyelectrolytes is quite effective on the structure of water. In contrast, zwitterionic monomer residues do not disturb the hydrogen bonding between water molecules.

Recently, Zhang et al. demonstrated that grafting or adsorption of sulfobetaine- or carboxybetaine-based polymers significantly reduced protein adsorption onto surfaces.<sup>21–25</sup> They reported that the surfaces were capable of resisting nonspecific protein

adsorption to a level comparable with well-packed oligo(ethylene glycol).<sup>24,26</sup> Recent studies attribute the nonfouling properties of oligo(ethylene glycol) to its strong hydration capability and well-packed structure.<sup>27–29</sup> Whereas hydrophilic and neutral oligo- or poly(ethylene glycol) form a hydration layer via hydrogen bonds, zwitterions form a hydration layer via electrostatic interactions.<sup>18</sup> It is expected that zwitterions are capable of binding significant quantities of water and are therefore potentially excellent candidates for nonfouling materials. Georgiev et al.<sup>30</sup> proposed an original theory for the explanation of the unique polyzwitterion nonbiofouling properties.

Assuming that ampholyte polymers, a special class of polyelectrolytes that contain both positive and negative charges along the macromolecular chain, do not disturb water structure, thus leading to a nonbiofouling surface,<sup>31</sup> other types of polyampholyte will possibly be candidates for nonbiofouling polymers. Considering that bovine serum albumin (BSA) is usually used as a nonbiofouling agent, amino acid-based polyampholytes may be useful agents. Some amino acid-based polyampholytes have been used in biomedical applications.<sup>32–34</sup> We have also already reported the biomedical applications of some amino acid-based polyampholytes and hydrogels.<sup>35,36</sup>

Here we designed an amino acid-based polyampholyte (a protein-mimicking polymer) that adsorbed onto a hydrophobic surface as the result of incorporation of a hydrophobic moiety into the polyampholyte. The polyampholyte consists of a weak acid (carboxylic acid) and a weak base (ammonium group) and, therefore, is different from other polyampholytes that have been previously reported, which are composed of strong acids, e.g., phosphoric acid<sup>7–20</sup> and sulfonic acid,<sup>21–23,25,37</sup> and strong bases, e.g., quaternary ammonium groups, for construction of a nonfouling surface. It was found that surfaces coated with such weak polyampholytes were very hydrophilic and efficiently inhibited adsorption of proteins and cells.

### Materials and Methods

**Materials.** L-Histidine (98%), methacryloyl chloride (97%), and 2,2'-azoisobutyronitrile (AIBN, 98%) were purchased from Wako Pure

\* To whom correspondence should be addressed.

† RIKEN.

‡ Kanagawa Academy of Science and Technology.

§ Università degli Studi di Siena.

|| Current address: Department of Bioengineering, Graduate School of Engineering, The University of Tokyo, 7-3-1 Hongo, Bunkyo-ku, Tokyo 113-8656, Japan.

Chemical Inc. (Osaka, Japan). AIBN was recrystallized from methanol. *n*-Butyl methacrylate was purchased from Kanto Chem. Inc. (Tokyo, Japan) and distilled under reduced pressure. All other chemical reagents were used as received. Bovine serum albumin was purchased from Sigma (St. Louis, MO). Lipidure was kindly provided by Nippon Oil (Tokyo, Japan).

**Synthesis of *N*-Methacryloyl-L-histidine (MHIs).** *N*-Methacryloyl-L-histidine (MHIs) was prepared according to the method previously reported by Okamoto.<sup>38</sup> L-Histidine (10 g, 64 mmol) was dissolved in 2 N NaOH (40 mL), and the aqueous solution was cooled in an ice bath. Methacryloyl chloride (7.3 mL, 76 mmol, 1.2 eq.) was dissolved in 20 mL of dioxane. The dioxane solution was added to the aqueous solution of L-histidine dropwise under a nitrogen atmosphere. During the addition, the reaction mixture was kept under 5 °C by external ice-bath cooling. After mixing, the solution was allowed to stand for 1 h at room temperature. After the reaction, the dioxane was evaporated and 6 N HCl was added until the solution reached pH 2. Unreacted chemicals and byproducts were removed by ether extraction. Subsequently, the pH of the aqueous solution was adjusted to 5 using 2 N NaOH, and the product was extracted with ethanol. By this process, L-histidine and NaCl were removed. The ethanol was removed and mixed with an excess of acetone to precipitate the product. The product was dissolved in ethanol and precipitated in acetone. The product was vacuum-dried overnight and MHIs was obtained. <sup>1</sup>H NMR (400 MHz, D<sub>2</sub>O): δ = 1.75 (s, 3H, CH<sub>3</sub>C(=CH<sub>2</sub>)H-), 2.95–3.23 (m, 2H, -CH<sub>2</sub>-imidazole), 4.41–4.46 (q, H, -NHCH(COOH)CH<sub>2</sub>-), 5.31–5.52 (m, 2H -CH<sub>2</sub>C(CH<sub>3</sub>-), 7.12 (s, 1H imidazole, -C=CHN=), 8.44 (s, 1H imidazole, -N=CHNH-).

**Polymerization.** Poly(*N*-methacryloyl-L-histidine) (PMHIs), poly(*n*-butyl methacrylate) (PBMA), and poly(*N*-methacryloyl-L-histidine-*co-n*-butyl methacrylate) (P(MHIs/BMA)) copolymer were synthesized by conventional free-radical polymerization. PMHIs was obtained as follows. The mixture of MHIs and/or BMA (the total monomer was adjusted to 0.5 mmol) in ethanol (20 mL) containing AIBN (0.05 mmol) was purged with N<sub>2</sub> gas and then allowed to react under N<sub>2</sub> atmosphere at 70 °C for 20 h. The polymer obtained was purified using seamless cellophane dialysis tubing (MWCO 3500) in distilled water or ethanol for 2 days and then lyophilized to give a white powder. All of the obtained polymers were dissolved in a methanol/0.1 N NaOH<sub>aq</sub> (9/1 vol) mixture. A 0.5 wt % solution was used for polymer coating.

**Polymer Characterization.** Size exclusion chromatography (SEC) measurements were carried out using a TSK gel column (TSKgel α-M, TOSOH, Tokyo, Japan) and an internal refractive index (RI) detector. For PMHIs, 0.1 M Tris buffer (pH 8.0, containing 0.2 M NaCl) was used as the eluent at a flow rate of 0.6 mL/min at 25 °C. For PBMA and P(MHIs/BMA), DMF containing 10 mM lithium bromide was used as the eluent at a flow rate of 0.6 mL/min at 25 °C. Commercially available poly(ethylene oxide) or polystyrene were used for the calibration of PMHIs and P(MHIs/BMA) or PBMA chromatography, respectively. <sup>1</sup>H NMR spectra were monitored using a JEOL EX400 (Akishima, Japan) spectrometer at 400 MHz in D<sub>2</sub>O or a D<sub>2</sub>O/CD<sub>3</sub>OD mixture. FT-IR spectra were monitored using a Shimadzu FTIR-8400S (Kyoto, Japan) equipped with an ATR attachment (Durasamp1 II, SensIR Tech., Danbury, CT).

**Adsorption of Polymers onto Surfaces.** To investigate the adsorption of polymers onto polystyrene surfaces, 0.1% (wt/v) polymer or BSA solution was added to 1.0 g of polystyrene beads (200–400 mesh) purchased from Tokyo Chem. Ind. Co., Ltd. (Tokyo, Japan) in test tubes. After vigorous shaking with a vortex mixer, the test tubes were centrifuged (1000 rpm, 5 min, r.t.) and the absorbance of the supernatant at 210 nm was measured. The amount of adsorbed polymer was estimated from a calibration curve.

**Contact Angle Measurement.** The static contact angles of air bubbles on the surfaces of polymer-coated substrates were measured with a contact angle meter DM 500 (Kyowa Interface Science, Saitama, Japan) at room temperature by the air-in-water method, which followed a captive bubble technique in which a sample film was immersed in

water and a small air bubble was placed onto the film from the surface using a curved needle. The polymer films were prepared as follows. The polymer solution was cast onto a nontreated polystyrene substrate and dried in air for 3 h. The substrate was rinsed with PBS solution and immersed in distilled water just prior to use. An air bubble (1 μL) was attached to the immersed substrate, and the contact angle was measured at least 5 times to give a reliable average value.

**Protein Adsorption.** Protein adsorption was measured by two methods. One was the measurement of decreases in protein solution concentrations following adsorption of proteins onto the surfaces. The other was direct observation of the protein adsorbed onto the plates.

For the former measurement, a Protein Detector ELISA kit (HRP/ABTS system) from Kirkegaard & Perry Lab., Inc. (Gaithersburg, MD) was used for the quantitative evaluation of nonspecifically adsorbed proteins on the polymer coated surface. In brief, the wells of nontreated 96-well plates were filled with each polymer solution and then emptied immediately, and the polymer-coated wells were air-dried. In the case of BSA, the wells were filled with 1.0% BSA solution and allowed to stand for 1 h. The coated wells were washed with 200 μL of PBS solution at least three times to completely remove nonadsorbed polymer, and then 100 μL of horseradish peroxidase-labeled anti-mouse immunoglobulin (HRP-IgG) solution (0.2 μg/mL) was added and allowed to stand for 1 h to adsorb onto the well surface. The wells were washed at least three times with 200 μL of wash solution containing 0.02% Tween, and then 50 μL of peroxidase substrate (2,2'-azino-bis(3-ethylbenzthiazoline-6-sulfonic acid, ABTS) reaction solution was added and allowed to react until color developed sufficiently. Then 50 μL of stop solution was added, and the absorbance of an aliquot of the solution was measured at 415 nm using a microplate reader (Bio-Rad model 680, Bio-Rad Laboratories, Tokyo, Japan).

For the latter measurement, a chemical luminescent imaging assay was employed. A total of 3 μL of a solution of horseradish peroxidase-linked bovine serum albumin in PBS (500 ng/mL, HRP-BSA, Rockland) was added to the noncoated or polymer-coated plates and allowed to stand for 15 min. Subsequently, the surfaces were washed twice with PBS for 3 min each time. The chemical luminescence reaction was performed with 10 μL of ECL advance solution (GE Healthcare) for 3 min at 20 °C. The reaction area was surrounded with liquid blocker (Daido Sangyo, Japan) to prevent the reaction solution from running over. The chemical luminescent images were measured using a Light Capture system (ATTO Corporation, Japan). Calibration was performed using HRP-BSA of known concentrations and ECL advance solution.

**Cell Culture.** Mouse osteoblast cells (MC3T3-E1) purchased from the RIKEN Cell Bank (Tsukuba, Ibaraki, Japan) were cultured on culture dishes (Corning Co., Ltd., Corning, NY) containing medium composed of minimum essential medium (MEM-α, Kohjin Bio Co. Ltd., Sakado, Japan) supplemented with 10% fetal bovine serum (FBS, BioWest, Nuaille, France) in a fully humidified atmosphere with a volume fraction of 5% CO<sub>2</sub> at 37 °C.

For the investigation of cell adhesion, 100 μL of each polymer solution was precoated onto each well of nontreated 12-well plates (IWAKI, Tokyo, Japan). They were then dried in air and rinsed twice with PBS. The cells were harvested with a 0.25% trypsin solution containing 0.5 mM EDTA. The recovered cells were then washed with culture medium and suspended in the medium. The cell suspensions were seeded at 4 × 10<sup>3</sup> cells/cm<sup>2</sup> onto polymer-precoated wells and allowed to stand for 5 h in a fully humidified atmosphere with a volume fraction of 5% CO<sub>2</sub> at 37 °C. After incubation, the number of adherent cells in a certain area was counted by microscopy.

To investigate the cytotoxicity of the polymers, the cells were cultured for 2 days and the cell number evaluated using a Cell Counting Kit (WST-1 method, Dojindo Lab., Kumamoto, Japan).<sup>39</sup> Briefly, after the MC3T3-E1 cells reached confluence, they were trypsinized and seeded at 1 × 10<sup>4</sup> cells/cm<sup>2</sup> into 96-well microplates (Corning Co., Ltd.) and then incubated for 2 days in a humidified atmosphere containing 5% CO<sub>2</sub> at 37 °C. After removing the cultured medium,

**Table 1.** Molecular Weights and Composition of Prepared Copolymers

| abbreviation    | MHis composition in feed (mol %) | $M_w$ ( $M_w/M_n$ )      | MHis composition in copolymer (mol %) |
|-----------------|----------------------------------|--------------------------|---------------------------------------|
| PMHis           | 100                              | $9.2 \times 10^4$ (2.54) | 100                                   |
| P(MHis/BMA)_7:3 | 70                               |                          | 72.0                                  |
| P(MHis/BMA)_5:5 | 50                               | $2.3 \times 10^4$ (2.33) | 50.1                                  |
| P(MHis/BMA)_3:7 | 30                               | $1.6 \times 10^4$ (2.22) | 28.7                                  |
| P(MHis/BMA)_1:9 | 10                               | $3.5 \times 10^4$ (1.90) | 8.6                                   |
| PBMA            | 0                                | $3.2 \times 10^4$ (1.76) | 0                                     |

100  $\mu\text{L}$  of MHis, PMHis, and P(MHis/BMA) solution (or suspension) in culture medium supplemented with 10% (v/v) FBS was added to each well and allowed to stand in a fully humidified atmosphere with a volume fraction of 5%  $\text{CO}_2$  at 37  $^\circ\text{C}$ . The MHis concentration of P(MHis/BMA) indicates the MHis monomer concentration in the polymer. After 24 h incubation, 10  $\mu\text{L}$  of WST-1 reagent was added to each well and incubated for 2 h at 37  $^\circ\text{C}$ , and then 10  $\mu\text{L}$  of 0.1 N HCl aqueous solution was added to each well to stop the reaction. To remove insoluble copolymer, the plate was centrifuged (1000 rpm, 5 min), and then 50  $\mu\text{L}$  of the supernatant was transferred to another plate. The absorbance of an aliquot of the solution was measured at 450 nm, with reference to the absorbance at 655 nm, using a microplate reader (Bio-Rad model 680).

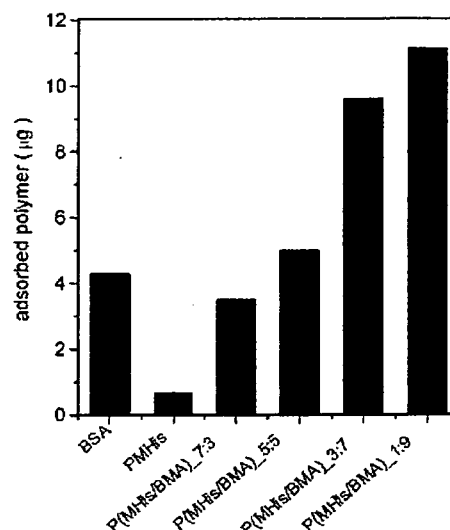
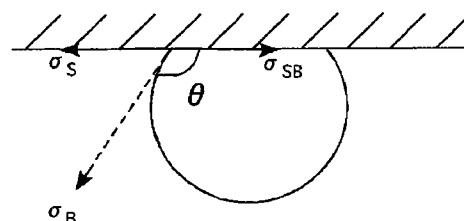
## Results and Discussion

**Polymer Properties.** The molecular weights and the chemical compositions of copolymers were measured by SEC and elemental analysis, respectively. The copolymer compositions were almost the same as the composition of the feed, and the molecular weights were as expected from the monomer/initiator ratios as shown in Table 1.

The solubilities of the copolymers were different from that of the homopolymer. Although the L-histidine homopolymer is only soluble in water, all of the copolymers including the homopolymer were soluble in a mixture of water and methanol. Because alcohol does not usually affect resin surfaces, it is a good solvent for coating polymers without significant influence on the surface properties of resins. Lipidure coating is also performed with alcohol. Considering these results, a methanol/water cosolvent (pH 12.4) was employed for further experiments.

**Coating with Polymers.** The polymers were solubilized in a mixture of water and methanol. Polystyrene beads were incubated in these solutions and the amounts of polymer adsorbed were determined as shown in Figure 1. The homopolymer PMHis hardly adsorbed onto the polystyrene beads. However, with increases in the *n*-butyl methacrylate composition, the amount of adsorbed polymer increased. These results indicate that the hydrophobic component of *n*-butyl methacrylate contributed to the adsorption of the polymers through their hydrophobicity. In the reported design of Lipidure, it was noted that *n*-butyl methacrylate was employed for enhancement of adsorption.<sup>10</sup> Chang et al.<sup>23</sup> reported diblock copolymer containing poly(sulfobetaine methacrylate) with poly(propylene oxide) as a hydrophobic moiety for coating material.

Table 2 shows the contact angles of air bubbles in water. The higher value of  $\theta$  indicates the higher hydrophilicity. Polymer adsorption significantly enhanced the hydrophilicity of the polystyrene surfaces. The enhancement effect of all copolymers was higher than that of BSA and was independent

**Figure 1.** Amounts of polymers adsorbed onto polystyrene beads (1 g). As PBMA does not have UV absorption, its adsorption was not measured.  $n = 3$ .**Table 2.** Contact Angles of the Polymer-Coated Substrate

| polymers for coating | coating solvent               | contact angle $\theta$ (deg) |
|----------------------|-------------------------------|------------------------------|
| none                 |                               | $117.6 \pm 5.5$              |
| PMHis                | methanol/0.1 N NaOH(aq) (9:1) | $138.9 \pm 2.7$              |
| P(MHis/BMA)_7:3      | methanol/0.1 N NaOH(aq) (9:1) | $165.0 \pm 1.1$              |
| P(MHis/BMA)_5:5      | methanol/0.1 N NaOH(aq) (9:1) | $162.8 \pm 1.2$              |
| P(MHis/BMA)_3:7      | methanol/0.1 N NaOH(aq) (9:1) | $163.6 \pm 0.7$              |
| P(MHis/BMA)_1:9      | methanol/0.1 N NaOH(aq) (9:1) | $163.6 \pm 1.8$              |
| PBMA                 | ethanol                       | $124.4 \pm 2.8$              |
| BSA                  | phosphate-buffered solution   | $151.5 \pm 7.3$              |
| Lipidure             | ethanol/water (1:1)           | $159.7 \pm 2.7$              |

of the MHis composition, although it was difficult to directly compare the effects of the coating materials because of the use of different coating solvents. This result indicates that the L-histidine residues significantly contributed to the hydrophilicity of the copolymers. The low effect of the homopolymer PMHis is considered to be due to low adsorption onto the surface.

**Nonfouling Properties.** Figure 2A shows HRP-IgG adsorption onto the polymer-coated resin. With copolymer coating, the adsorption of HRP-IgG was significantly reduced. In particular, the copolymer containing 50% histidine almost completely inhibited nonspecific adsorption of IgG. The lower nonfouling effect of PMHis was considered to be the low coverage of the surface and resulted low hydrophilicity. To investigate this result in detail, the enzyme reaction time was increased and the effect was enhanced as shown in Figure 2B. The reduction effect was higher than for BSA or Lipidure, which are usually employed for reduction of nonspecific adsorption of proteins in enzyme-linked immunosorbent assays (ELISA).

Figure 3 shows the direct observation by chemical luminescence of adsorbed HRP-BSA on polystyrene plates. The protein

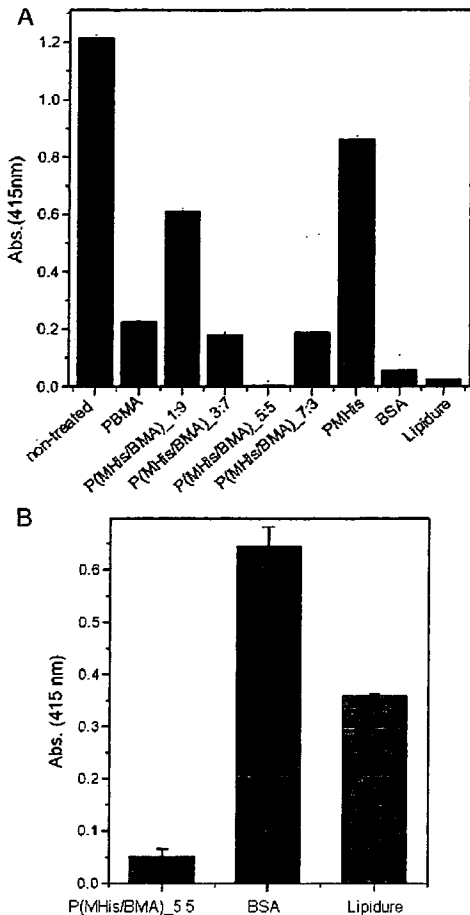


**Figure 2.** Adsorption of HRP-IgG onto non- or polymer-coated polystyrene plates. Incubation times were 5 (A) and 120 min (B). *n* = 3.

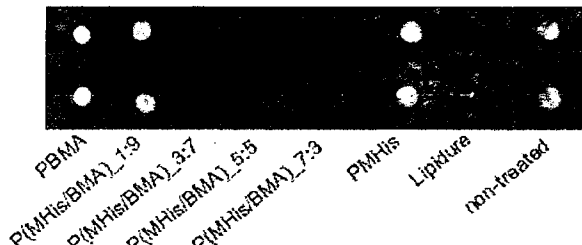


**Figure 3.** Chemical luminescence images of HRP-BSA on non- or polymer-coated polystyrene plates.

was highly adsorbed on unmodified, PBMA-coated, and PMHis-coated plates. However, on the copolymer containing a high content of MHis, the adsorption was significantly less. The protein adsorption was quantitatively evaluated and is shown in Figure 4. Although it is very difficult to directly compare the results in Figures 2 and 4, because of the differences in proteins and experimental conditions, it was concluded that the copolymer containing the higher content of MHis apparently reduced protein adsorption, comparable to using Lipidure or BSA.

Figure 5 shows photos of cells adhered on various surfaces. The ratio of round-shaped cells to spread ones was higher on the copolymer-coated surfaces than on the nontreated or BSA-coated surfaces. In the comparison with Lipidure-coated surfaces, no spreading cells were found on the P(MHis/BMA)\_5:5-coated surfaces. These round cells were easily washed away.

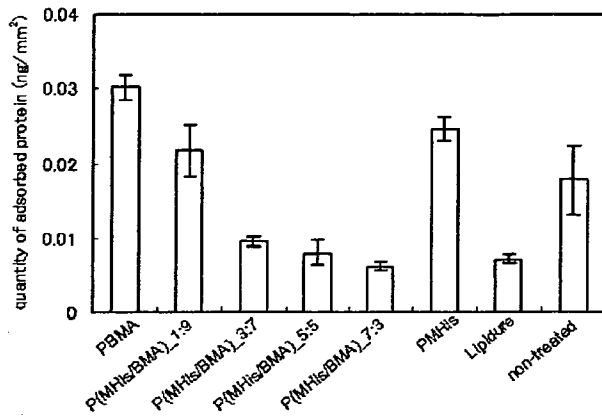


**Figure 4.** Amount of HRP-BSA adsorbed on non- and polymer-coated polystyrene plates. *n* = 3.

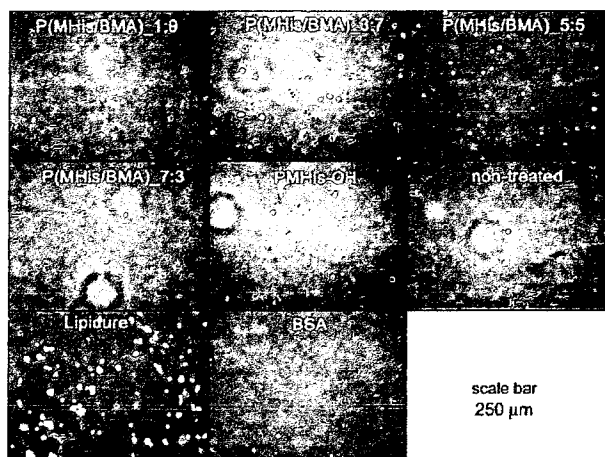


**Figure 5.** Phase contrast micrographs of adherent cells on polymer-coated polystyrene plates for 5 h.

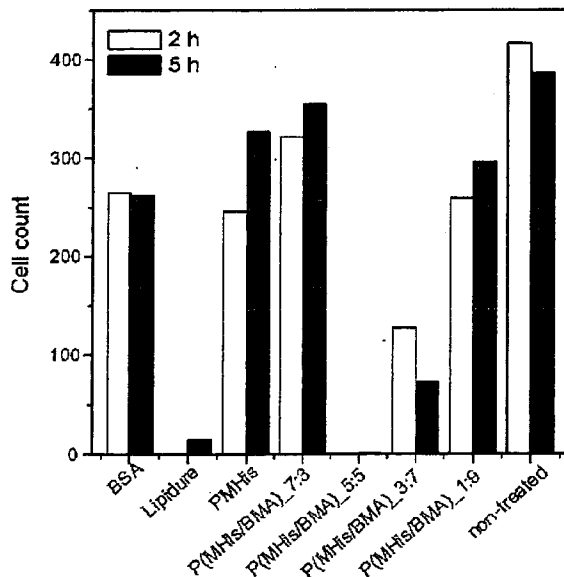


**Figure 6.** Number of cells adherent on polymer-coated polystyrene plate (cells/mm<sup>2</sup>). *n* = 3.

Therefore, the copolymer containing 50% histidine almost completely inhibited the adhesion of cells, as shown in Figure 6, an effect comparable to that of Lipidure. No cell adhesion was observed on P(MHis/BMA)\_5:5-coated surfaces, even after

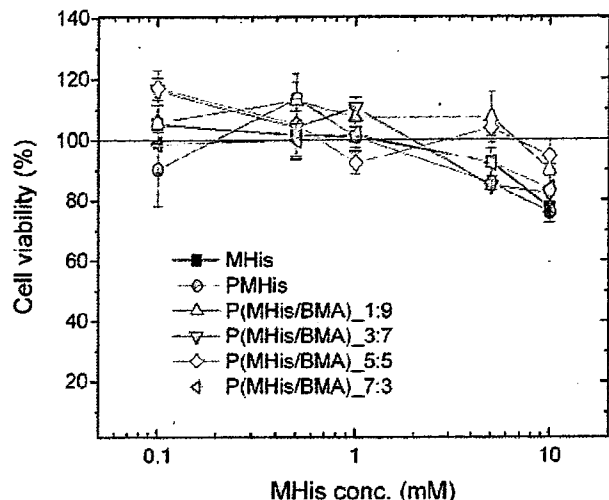


**Figure 7.** Viability of cells cultured in the presence of polymers for 2 days.  $n = 3$ .

5 h. The copolymers containing smaller ratios of histidine did not have adequate inhibitory effects.

**Cytotoxicity.** To evaluate the cytotoxicity of the prepared polymers, cell culture was performed in the presence of the polymers. We have already reported no cytotoxicity for polymers containing histidine residues.<sup>35,36</sup> Here we also found no significant cytotoxicity of these new polymers up to 5 mM, as shown in Figure 7.

In comparison with nonbiofouling polyampholytes carrying phosphatidylcholine residues investigated by other researchers,<sup>7–20</sup> the copolymers that were synthesized in this investigation had weak acid and base groups. However, similar or greater effects were observed for our polymers. As our polymer is based on an amino acid, this mild zwitterion polymer will be important as a new nonbiofouling polymer.

### Conclusion

This study demonstrated the synthesis of alcohol-soluble polyzwitterions by the copolymerization of *N*-methacryloyl-L-histidine and a hydrophobic monomer. Coating with the copolymer enhanced hydrophilicity and was efficient for the preparation of nonbiofouling surfaces active against protein and cell adhesion. In particular, the copolymer containing about 50% content of histidine monomer was the most suitable candidate for nonfouling for both proteins and cells. In addition, the copolymer was nontoxic. Therefore, the copolymer will be useful as a new nonbiofouling agent.

### References and Notes

- Harris, J. M.; Zalipsky, S. American Chemical Society, Division of Polymer Chemistry Meeting. *Poly(ethylene glycol): Chemistry and Biological Applications*; American Chemical Society: Washington, DC, 1997.
- Ratner, B. D.; Hoffman, A. S.; Schoen, F. J.; Lemons, J. E. *Biomaterials Science*, 2nd ed.; Elsevier Academic Press: San Diego, CA, 2004; p 197.
- Zhang, Z.; Ma, H.; Hausner, D. B.; Chilkoti, A.; Beebe, T. P., Jr. *Biomacromolecules* **2005**, *6*, 3388–3396.
- Ito, Y.; Hasuda, H.; Sakuragi, M.; Tsuzuki, S. *Acta Biomater.* **2007**, in press.
- Zhu, J.; Marchant, R. E. *Biomacromolecules* **2006**, *7*, 1036–1041.
- Higuchi, A.; Aoki, N.; Yamamoto, T.; Gomei, Y.; Egashira, S.; Matsuoka, Y.; Miyazaki, T.; Fukushima, H.; Jyujoji, S.; Natori, S. H. *Biomacromolecules* **2006**, *7*, 1083–1089.
- Ishihara, K.; Aragaki, R.; Ueda, T.; Watanabe, A.; Nakabayashi, N. *J. Biomed. Mater. Res.* **1990**, *24*, 1069–1077.
- Kojima, M.; Ishihara, K.; Watanabe, A.; Nakabayashi, N. *Biomaterials* **1999**, *12*, 121–124.
- Ishihara, K.; Ziats, N. P.; Tierney, B. P.; Nakabayashi, N.; Anderson, J. M. *J. Biomed. Mater. Res.* **1991**, *25*, 1397–1407.
- Ishihara, K.; Oshida, H.; Endo, Y.; Watanabe, A.; Ueda, T.; Nakabayashi, N. *J. Biomed. Mater. Res.* **1993**, *27*, 1309–1314.
- Ishihara, K.; Tsuji, T.; Kurosaki, T.; Nakabayashi, N. *J. Biomed. Mater. Res.* **1994**, *28*, 225–232.
- Ishihara, K.; Nomura, H.; Mihara, T.; Kurita, K.; Iwasaki, Y.; Nakabayashi, N. *J. Biomed. Mater. Res.* **1998**, *39*, 323–330.
- Lewis, A.; Hughes, P.; Kirkwood, L.; Leppard, S.; Redman, R.; Tolhurst, L.; Stratford, P. *Biomaterials* **2000**, *21*, 1847–1859.
- Lewis, A.; Cumming, Z.; Goreish, H.; Kirkwood, L.; Tolhurst, L.; Stratford, P. *Biomaterials* **2001**, *22*, 99–111.
- Willis, S.; Court, J.; Redman, R.; Wang, J.; Leppard, S.; O'Byrne, V.; Small, S.; Lewis, A.; Jones, S.; Stratford, P. *Biomaterials* **2001**, *22*, 3261–3272.
- Nakabayashi, N.; Williams, D. *Biomaterials* **2003**, *24*, 2431–2435.
- Feng, W.; Brash, J. L.; Zhu, S. *Biomaterials* **2006**, *27*, 847–855.
- Chen, S.; Zheng, J.; Li, L.; Jiang, S. *J. Am. Chem. Soc.* **2005**, *127*, 14473–14478.
- Kitano, H.; Sudo, K.; Ichikawa, K.; Ide, M.; Ishihara, K. *J. Phys. Chem. B* **2000**, *104*, 11425–11429.
- Kitano, H.; Imai, M.; Mori, T.; Gemmei-Ide, M.; Yokoyama, Y.; Ishihara, K. *Langmuir* **2003**, *19*, 10260–10266.
- Zhang, Z.; Chen, S.; Chang, Y.; Jiang, S. *J. Phys. Chem. B* **2006**, *110*, 10799–10804.
- Zhang, Z.; Chao, T.; Chen, S.; Jiang, S. *Langmuir* **2006**, *22*, 10072–10077.
- Chang, Y.; Chen, S.; Zhang, Z.; Jiang, S. *Langmuir* **2006**, *22*, 2222–2226.
- Zhang, Z.; Chen, S.; Jiang, S. *Biomacromolecules* **2006**, *7*, 3311–3315.
- Chang, Y.; Chen, S.; Yu, Q.; Zhang, Z.; Bemards, M.; Jiang, S. *Biomacromolecules* **2007**, *8*, 122–127.
- Li, L.; Chen, S.; Zheng, J.; Ratner, B. D.; Jiang, S. *J. Phys. Chem. B* **2005**, *109*, 2934–2941.
- Harder, P.; Grunze, M.; Dahint, R.; Whitesides, G. M.; Laibinis, P. E. *J. Phys. Chem. B* **1998**, *102*, 426–436.
- Ostuni, E.; Chapman, R. G.; Holmlin, R. E.; Takayama, S.; Whitesides, G. M. *Langmuir* **2001**, *17*, 5606–5620.
- Zheng, J.; Li, L.; Tsao, H.-K.; Sheng, Y.-J.; Chen, S.; Jiang, S. *Biophys. J.* **2005**, *89*, 158–166.
- Georgiev, G. S.; Kamenska, E. B.; Vassileva, E. D.; Kamenova, I. P.; Georgieva, V. T.; Iliev, S. B.; Ivanov, I. A. *Biomacromolecules* **2006**, *7*, 1329–1334.
- Kudaibergenov, S. E., Ed.; *Polyampholytes: Synthesis, Characterization and Application*; Kluwer Academic: New York, 2002.
- Ihm, J.-E.; Han, K.-O.; Han, I.-K.; Ahn, K.-D.; Han, D.-K.; Cho, C.-S. *Bioconjugate Chem.* **2003**, *14*, 707–708.
- Lele, B. S.; Kulkarni, M. G.; Mashelkar, R. A. *React. Funct. Polym.* **1999**, *40*, 215–229.
- Langer, R.; Putnam, D. A. U.S. Patent 6,849,272, 2005.
- Casolaro, M.; Bottari, S.; Cappelli, A.; Mendichi, R.; Ito, Y. *Biomacromolecules* **2004**, *5*, 1325–1332.
- Casolaro, M.; Bottari, S.; Ito, Y. *Biomacromolecules* **2006**, *7*, 1439–1448.
- Olenych, S. G.; Moussallem, M. D.; Salloum, D. S.; Schlenoff, J. B.; Keller, T. C. *Biomacromolecules* **2005**, *6*, 3252–3258.
- Okamoto, Y. *Nippon Kagaku Kaishi* **1978**, *6*, 870–873.
- Ishiyama, M.; Tominaga, H.; Shiga, M.; Sasamoto, K.; Ohkura, Y.; Ueno, K. *Biol. Pharm. Bull.* **1996**, *19*, 1518–1520.

BM070420H